β-delayed neutron emission in the ^{78}Ni region

I. N. Borzov
University of Leuven, B-3001 Leuven, Belgium
(Received 9 September 2004; revised manuscript received 26 January 2005; published 13 June 2005)

A systematic study of the total β-decay half-lives and β-delayed neutron emission probabilities is performed. The β-strength function is treated within a self-consistent density-functional + continuum-quasiparticle-random-phase-approximation framework including the Gamow-Teller and first-forbidden transitions. The experimental total β-decay half-lives for the Ni isotopes with $A \leqslant 76$ are described satisfactorily. The half-lives predicted from $A = 70$ up to $A = 86$ reveal fairly regular A behavior which results from simultaneous account for the Gamow-Teller and first-forbidden transitions. For $Z \approx 28$ nuclei, a suppression of the delayed neutron emission probability is found when the $N = 50$ neutron closed shell is crossed and the neutron excess becomes more than one major shell. The effect originates from the high-energy first-forbidden transitions to the states outside the Q_β-B_n window in the daughter nuclei.

DOI: 10.1103/PhysRevC.71.065801 PACS number(s): 23.40.Bw, 21.60.Jz, 26.30.+k, 27.50.+e

I. INTRODUCTION

Physics of complex nuclear systems with high isospin asymmetry is a rich and multifaceted field. It involves such exotic objects as neutron stars and short-lived β-unstable nuclei with a large neutron (proton) excess. The ground state and β-decay properties of these radioactive isotopes give valuable information on structural evolution in the regions far-off stability and provide input for supernova explosion calculations. In particular, for the modeling of the r-process nucleosynthesis, the most important objects are the nuclear masses that define the path of the r process through the neutron-rich domain of the nuclear chart. The β decays and $\nu(\bar{\nu})$ captures are also essential, as they regulate the flow of the material to high Z values and set up the r process time scale. The nuclei near the new doubly magic ^{78}Ni and ^{132}Sn, as well as the very neutron-rich nuclei "east" of ^{208}Pb are of special importance to the r process modeling. Some of the key nuclei in these regions have been reached recently thanks to the spectacular progress of the Radioactive Nuclear Beams (RNB) experiments using the Z-selective resonance-ionization laser ion-source technique (see, e.g. [1]). It has provided a unique testing ground for theoretical approaches to exotic nuclei and modeling of explosive stellar events.

In this paper, we perform the microscopic study of the total β-decay half-lives and β-delayed neutron emission probabilities of very neutron-rich nuclei. The simultaneous analysis of these β-decay observables may make it possible to reconstruct the β-strength function. Specifically, one may gain insight into the relative contribution of its Gamow-Teller (GT) and first-forbidden (FF) components. A possibility of competition between the GT and FF decays in nuclei with the neutron-excess bigger than one major shell has often been discussed in the literature (see [2] and references therein). Experimental evidence of that has been obtained since the first measurements in the region of ^{132}Sn [3]. However, microscopic global calculations [4,5] have treated the total β-decay half-lives and delayed neutron emission probabilities P_n in allowed transition approximation. Moreover, contrary to [2], Ref. [4] stated that the influence of forbidden decays should decrease with increasing distance from the valley of β stability. Later, the microscopic study of the unique FF transitions [6] came to the conclusion that even this simplest forbidden decay channel (which is important in a number of special cases) should be taken into account.

The single β-decay channel approximation is not adequate for describing of the isotopic dependence of the β-decay characteristics, especially for the nuclei crossing the closed N and Z shells. It has been pointed out recently in [7] that self-consistent framework of the finite Fermi system theory that includes the GT and FF decays on the same footing allows for reasonably sound predictions of the ground state properties and β-decay characteristics of very neutron-rich nuclei. An important contribution of the FF nonunique decays to the total half-lives of neutron-rich nuclei above the closed proton and neutron shells has been stressed in [7,8]. The aim of this work is to examine the impact of high-energy FF decays on the β-delayed neutron emission in a wide region of nuclei near the closed shells at $Z = 28$ and $N = 50$. The structure of the paper is the following. In Sec. II, we briefly outline the particulars of a theoretical framework based on the density functional (DF) approach and the continuum quasiparticle random phase approximation (CQRPA). New calculations of the total β-decay half-lives and β-delayed neutron emission probabilities are presented in Sec. III. Analysis of possible uncertainties is also given. In conclusion, Sec. IV relates the results to current experimental studies.

II. THEORETICAL ANALYSIS

A. β-decay characteristics

The β-delayed neutron emission is basically a multistep process consisting of (a) the β-decay of the precursor (A, Z) which results in feeding the excited states of the emitter nucleus $(A, Z + 1)$ followed by the (b) γ deexcitation to the ground state or (c) neutron emission to an excited state or to the ground state of the final nucleus $(A - 1, Z + 1)$. The difference in the characteristic time scales of the β

decay and subsequent particle emission processes justifies an assumption of their statistical independence. Within the β-strength function formalism, the total probability of the delayed neutron emission accompanying the β decay to the excited states in the daughter nucleus can be expressed as [9]

$$P_n = T_{1/2} D^{-1} (G_A/G_V)^2 \int_{B_n(Z+1)}^{Q_\beta} d\omega f_0(Z+1, A, \omega) \times \sum_\beta \langle \kappa_J \rangle S_\beta(\omega, \gamma) P\left(j^\pi{}_{i,f}, E_n\right), \quad (1)$$

where $T_{1/2}$ stands for total β-decay half-life

$$1/T_{1/2} = D^{-1} (G_A/G_V)^2 \int_0^{Q_\beta} d\omega f_0(Z+1, A, \omega) \times \sum_\beta \langle \kappa_J \rangle S_\beta(\omega, \gamma), \quad (2)$$

where $D = 6163.4 \pm 3.8$ s, with $G_V = (1.4130 \pm 0.0004) \times 10^{-49}$ erg cm^3, $G_A/G_V = 1.26$, $B_n(Z+1)$ is a neutron emission threshold of the emitter, and Q_β is a total β-decay energy. The β-strength functions $S_\beta(\omega, \gamma)$ describe the spectral distributions of the matrix elements of the GT and FF β-decay transitions to the emitter nucleus. The energy of the β-decay transition between the ground state of the parent nucleus and excited state of the emitter is $\omega = W + E_{\tilde{\nu}}$, where W, $E_{\tilde{\nu}}$ are the emitted electron and antineutrino energies, respectively (the nuclear recoil energy and the neutrino mass are neglected); $\gamma = \Gamma^\downarrow + \Gamma^\uparrow$ is the total width of the isobaric excitation, which includes its escape and spreading widths. The index β in the sum corresponds to the GT term with $L = 0$, $J = 1$ and nonunique FF terms with $L = 1$, $J = 0, 1$ treated in the ξ approximation. The unique $J = 2$ term can be also retained, but in the ξ approximation it should be of minor importance. For the GT and nonunique FF decays $\langle \kappa_{J=0,1} \rangle = 1$, and for the unique FF decays, $\langle \kappa_{J=2} \rangle = f_1/f_0$, with the Fermi integral f_1 calculated as in [10]. $P(j^\pi{}_{i,f}, E_n)$ is the particle emission probability from the level $|j_i^{\pi_i}\rangle$ of the emitter to the level $|j_f^{\pi_f}\rangle$ of the final nucleus, E_n being the emitted neutron energy. The distorted lepton $(e^-, \tilde{\nu}_e)$ phase-space volume for allowed transitions (at the moment of the β decay) is given by

$$f_0(Z, A, \omega) = \int_{m_e c^2}^{\omega} F(Z, A, W) p W (\omega - W)^2 dW, \quad (3)$$

where the Fermi function $F(Z, A, W)$ depending on the charge number of the emitter nucleus includes the effect of the electron screening of the nuclear Coulomb field and finite-size corrections due to the extended nuclear charge distribution [11] (the electromagnetic corrections are not included).

If the β-decay transition energy relative to the mother nucleus ground state satisfies $\omega < Q_\beta - B_n \equiv Q_{\beta n}$, the neutron decaying state $|j_i^\pi\rangle$ is located within the so-called $Q_{\beta n}$ window in the particle continuum. Neglecting the γ deexcitation, the energy of the emitted neutron is $E_n = Q_\beta - B_n - \omega$. The particle emission probability from the level $|j_i^{\pi_i}\rangle$ of the emitter to the level $|j_f^{\pi_f}\rangle$ of the final nucleus, as a function of the emitted neutron energy E_n is given by

$$P\left(j^\pi{}_{i,f}, E_n\right) = \frac{\Gamma_n\left(j^\pi{}_{i,f}, E_n\right)}{\Gamma_n\left(j^\pi{}_{i,f}, E_n\right) + \Gamma_\gamma\left(j^\pi{}_{i,f}, E_\gamma\right)}, \quad (4)$$

where $\Gamma_n(j^\pi{}_{i,f}, E_n)$ is the neutron escape width and $\Gamma_\gamma(j^\pi{}_{i,f}, E_\gamma)$ is the γ-ray width of the emitter. These can be expressed through the transmission coefficients for the l-wave neutron emission with the total angular momentum j_n and corresponding γ-transmission coefficients calculated from the statistical model of Hausser-Feshbach. In what follows, we will assume that the γ emission from neutron-unbound states is absent: $\Gamma_\gamma \ll \Gamma_n$. The approximation $P = 1$ simplifies the calculations but may cause some overestimation of the resulting P_n values.

The strength functions in Eqs. (1) and (2) are calculated on the energy mesh; their maxima $S_\beta(\omega_i)$ are related to the intensities of the β-decay transitions to the states of the emitter nucleus. Actually, the half-life $T_{1/2}$ in Eq. (2) depends on the transition energy ω through $S_\beta(\omega)$. (A direct dependence on the Q_β value arises in the special case of the ground state to ground state transition.) The transition energies for the main GT and FF decays reveal a smooth A dependence, which simplifies the analysis substantially. An external variable Q_β is needed to "derive" the excitation energy in the daughter nuclei E_x, which has been used sometimes to define a total half-life [4,5]. In the non-self-consistent approaches with empirical mean-field potentials, the total β-decay energy is not defined. In this case, using the relation $E_x = Q_\beta - \omega$, one introduces an additional ("outer" [4]) parameter which, for instance, may change the isotopic behavior of the total half-lives.

B. DF+CQRPA

Below we outline the continuum-QRPA framework based on the self-consistent ground state description within the local energy-density functional theory. (For a detailed description see [7,12].) The ingredients of the approach are the self-consistent mean-field potential (for the ground state properties) and universal effective *NN* interaction (for description of the excited states); ideally, both originate from the unique nuclear energy-density functional. So far, some restrictions exist in applications of the fully self-consistent approach to nuclear spin excitations. In the Landau limit, the parameter of the particle-hole interaction g' derived from the available Skyrme density functionals turns out to be much lower than its empirical value. The satisfactory spin-dependent DFs have not been developed yet for spin-unsaturated nuclei [13].

In practice, the ground state properties are rather insensitive to the spin and spin-isospin dependent components of the DF (except for the spin-orbit term). Thus, the scalar and spin-isospin components of the DF can be decoupled, and the effective *NN* interactions in the scalar and spin-isospin channels can be introduced independently [12]. Thus, the DF+QRPA approach developed in such an approximation may gain an advantage of using in the *ph* channel the well-founded spin-isospin effective *NN* interaction of the finite Fermi system theory (FFS) [14] consisting of the Landau-Migdal contact

term augmented by the π and ρ exchange terms renormalized by nuclear medium. An important feature of the FFS is that the effective *NN* interactions in the particle-hole (*ph*) and particle-particle (*pp*) channels are not interconnected, as in the standard QRPA, but introduced independently. The *ph* interaction is assumed to be universal (*A* independent), which is of prime importance for the large-scale applications. In the DF+CQRPA approach, the Landau-Migdal constant of g' is very close to the empirical value, thereby ensuring a reliable description of the GT strength function in the whole energy scale including the continuum. The *pp* interaction of the FFS allows for a good description of the spin-isospin excitations in the region far from the QRPA instability point.

1. Ground state characteristics

To describe the ground state characteristics of the nuclei with pairing, the Fayans phenomenological DF [13] is adopted. It is characterized by the effective nucleon mass $M^* = 1$ and consists of a normal and a pairing part. Using the bare nucleon effective mass allows one to achieve a good description of the available single-particle levels both in stable and unstable nuclei. This description is indispensable to the correct estimation of the upper limit of the β-decay energy release. In particular, the DF3 version of the functional [12] contains also the two-body spin-orbit and velocity-dependent effective *NN* interactions important to the full consistency, as well as the isovector spin-orbit force. The latter ensures a correct description of the single-particle levels in nuclei near doubly magic ^{132}Sn [15]. We have also studied the possibility of using the ground state description given by the Skyrme MSk7 force [16].

The procedure for finding the quasiparticle energies and wave functions corresponds to a self-consistent Hartree-Fock (HF)-BCS scheme. The pairing energy density depends on the anomalous nucleon density ν, as $\varepsilon_{\text{pair}} = \frac{1}{2}\nu F^{\xi}\nu$. In a general case, the isotriplet ($T = 1$) effective *NN* interaction in the *pp* channel describing the pairing in the ground state has a contact density-dependent form: $F^{\xi}(\vec{r_{12}}) = -2C_0^{-1} f^{\xi}(x)\delta(\vec{r_{12}})$, where $\delta(x)$ is the Dirac delta function. Here and below, the normalizing factor $2C_0 = 600$ MeV fm^3 is the inverse half density of states at the Fermi surface in equilibrium nuclear matter. The $f^{\xi}(x)$ is a dimensionless strength treated in the local density approximation as a (local) functional of the isoscalar density $x = (\rho_p + \rho_n)/2\rho_0$, where the $\rho_{p,(n)}$ are the proton (neutron) densities; the $f^{\xi}(x)$ is expressed in a Skyrme-like form [13]. A local cutoff treatment of the pairing energy density [13] or regularization procedure [17] helps avoid the problem of the cutoff energy choice. Assuming the pairing potential $\Delta(r)$ is a smooth function of the spatial coordinates, the diagonal approximation $\Delta_{\lambda\lambda'} = \Delta_{\lambda}\delta_{\lambda\lambda'}$ is used (λ is the set of single-particle quantum numbers, $\delta_{\alpha\beta}$ being the Kroneker symbol). For the *pp* basis confined by the $\varepsilon_{\text{cut-off}} = 15$ MeV, the slightly *A*-dependent pairing strength parameter $f^{\xi} = 0.40$–0.33 is found to reproduce the empirical matrix elements of the proton (neutron) pairing potentials Δ^{τ} in the region of $A = 40$–220. For odd-*A* nuclei, the blocking of pairing by the odd quasiparticle is taken into account, as well as the rearrangement effects.

Thus, the nuclear binding energy as well as the quasiparticle level energies and occupancies are calculated within one and the same self-consistent HF-BCS procedure. The neutron emission threshold of the emitter $B_n(Z+1)$ and total β-decay energy Q_{β} are found as the atomic mass difference of parent and daughter nuclei [12]:

$$Q_{\beta} = B_{\text{nucl}}(Z, A) - B_{\text{nucl}}(Z+1, A) + m(nH), \quad (5)$$

$$B_n = B_{\text{nucl}}(Z+1, A) - B_{\text{nucl}}(Z+1, A+1) + m(n), \quad (6)$$

where $B_{\text{nucl}}(Z, A)$ is the calculated nuclear binding energy of the nucleus (Z, A) and $m(nH) = 0.782$ MeV, $m(n) = 8.071$ MeV.

2. β-strength function

To find the β-strength functions, the C-QRPA-like equations of the FFS are solved. They describe the effective fields induced in the nuclei by the β-decay driving operators. The approach is based on exact treatment of the *ph* continuum and the pairing and effective *NN* interactions in the *ph* and *pp* channels [18] . A full system of the continuum-QRPA equations is thus characterized by the SO(8) symmetry. Neglecting the effective *pp* interaction, as was done, e.g., in [5], would destroy the symmetry of the QRPA equations and cause unrealistic odd-even staggering of total β-decay half-lives. Notice, that for odd-*A* nuclei, the FFS equations account properly for the odd-particle transitions [19].

The method to include the *ph* continuum for the $\Delta T = 1$ excitations of superfluid nuclei [18,20] is similar to the one for $\Delta T = 0$ excitations [21]. It is based on the exact treatment of the pairing in "valence λ space" ($\mu^{\tau} - \xi < \varepsilon_{\lambda} < \mu^{\tau} + \xi$), where μ^{τ} are the neutron and proton chemical potentials. Far from the Fermi surface, the *ph* propagator is the same as in the system with no pairing. It is calculated via the Green functions constructed in the *r* space which allows the exact inclusion of the *ph* continuum. Thus, for the states above the neutron separation energies $B_n(Z+1)$ the escape width to the particle continuum $\Gamma^{\downarrow}$ naturally arises. To simplify the calculations of the β-decay half-lives, the spreading width of the isobaric states $\Gamma_{\downarrow}$ can be introduced. It is assumed to depend linearly on the excitation energy [22]. The cutoff at $\Delta\omega = 2.5\Gamma_{\downarrow}$ is employed for the high-energy wings of the individual excitations with $\omega \leqslant Q_{\beta}$.

To find the strength functions of the GT and FF β decays, the effective fields have to be found as a nuclear response to the following operators $\vec{\sigma}$, γ_5, $[\vec{\sigma}\vec{r}]^{(0)}$, α, $\vec{r}$, $[\vec{\sigma}\vec{r}]^{(1)}$, $[\vec{\sigma}\vec{r}]^{(2)}$ acting in the isospin space. Here $\vec{\sigma}$ are the Pauli spin matrices, and the rank of the tensor operators $[\vec{\sigma}\vec{r}]^{(J)}$ is defined by the momentum $|J_i - J_f| \leqslant J \leqslant |J_i + J_f|$ transferred to the emitter nucleus. Allowed and unique transitions involve only single β moments, while the β rates of the nonunique decays are determined by the incoherent contributions of different β moments. Besides, for $J = 0, 1$ transitions, the relativistic vector operator α and axial charge operator γ_5 should be included along with the spacelike operators.

To calculate the β-decay half-lives, the following external fields $\hat{V}^{(0)} = 2\sqrt{\pi}V^0_{JLS}\tau^-$ should be considered:

$$V^0_{1,0,1} = e_{qs}\vec{\sigma}\cdot\vec{\tau}\ , \tag{7}$$

for the Gamow-Teller transitions, and

$$\begin{aligned} V^0_{0,1,1} &= e_{qs}i\vec{\sigma}\cdot\vec{r} - e_{q5}\vec{\sigma}\cdot\vec{P}/2M, \\ V^0_{1,1,0} &= \frac{1}{\sqrt{3}}(i\vec{r} - \vec{P}/2M), \\ V^0_{1,1,1} &= e_{qs}\sqrt{2}[\vec{\sigma}\vec{r}]^{(1)}, \\ V^0_{2,1,1} &= e_{qs}\frac{2}{\sqrt{3}}[\vec{\sigma}\vec{r}]^{(2)}, \end{aligned} \tag{8}$$

for the first-forbidden transitions (α, γ_5 are taken in the nonrelativistic limit). The normalization of the space-dependent external fields V^0_{JLS} is the one accepted in [23].

3. Reduction of the velocity-dependent β moments

To avoid using the velocity-dependent fields, an efficient approximation is to replace α, γ_5 by the space-dependent fields [7]. The exact nonrelativistic relation for the matrix element of the timelike operator $\langle\alpha\rangle = \xi/\lambda_e\cdot\Lambda_1\cdot\langle i\vec{r}\rangle$ can be applied which reflects the conservation of the nuclear vector current (CVC). In a fully self-consistent approach, a precise cancellation takes place of all the terms except the averaged Coulomb potential, thus the translation factor Λ_1 reads $\xi\Lambda_1 = \omega_{if} + \bar{u}_C$ where ω_{if} is the transition energy and $\bar{u}_C$ is the Coulomb potential averaged over the neutron excess. For the timelike operator γ_5 and its spacelike counterpart $\vec{\sigma}\cdot\vec{r}$, no analogous exact relation exists due to the partial conservation of the axial-vector current (PCAC). The self-consistent FFS sum rule approach [24] is used to approximate the operator γ_5 in an analogous way by the spacelike operator $\vec{\sigma}\cdot\vec{r}$, taking into account the medium corrections which are mainly due to the spin-orbit and velocity-dependent interactions [7]. With the space-dependent external fields, the GT+FF calculations of the β rates are feasible.

The universal medium renormalization of the external fields of a different symmetry (beyond the QRPA-type correlations) is taken into account via the quasiparticle local charge operators $\hat{e}_{qi} = e_q[V_0^{JLS}]$. The "quenching factor" $Q = e_{qs}[\sigma\tau]^2 = (g_A/G_A)^2$ suppresses the spin-isospin fields in the nuclear medium. The smaller the Q, the less strength contained in the low-energy part ($\omega < \varepsilon_F$) of the spin-isospin response, and therefore the shorter the β-decay half-lives. From the chiral symmetry and soft-pion limit, it follows that $\langle\gamma_5\rangle$ vertex is substantially amplified in the nuclear medium due to the meson-exchange currents and the effective *NN* interactions [25]. Thus, the $\vec{\sigma}\cdot\vec{P}$ field is renormalized by the FFS axial local charge $e_{q5} = e_q[\gamma_5]$; as in [26], we use $e_{q5} = 1.5$.

4. Effective NN interaction

In the effective *NN* interaction for β-decay studies, the appropriate balance of the short- and finite-range components should be maintained, as well as the balance of repulsive and attractive parts. In the *ph* channel, the effective *NN* interaction is chosen in a $\delta + \pi + \rho$ form. The first repulsive term corresponds to the contact interaction with the Landau-Migdal constant g'. The attractive terms corresponding to the one-π exchange (g_π) and one-ρ exchange (g_ρ) modified by the nuclear medium are important in describing the magnetic properties of nuclei and the nuclear spin-isospin responses. The competition of repulsion and attraction determines a degree of "softness" of the pionic modes in nuclei that directly affects the β-decay half-lives. The set of the *NN* interaction parameters $g' = 0.98$, $g_\pi = -1.38$, $g_\rho = -1.04$ has been used, corresponding to the GT quenching factor of the spin-isospin response function $Q = e_q[\sigma\tau]^2 = 0.81$ (see [7]). It was derived from the description of nuclear magnetic moments which allows for moderately soft π modes [27]. The recent analysis of (p, n) reaction spectra at $E_p = 295$ MeV [28] and excitation energies up to $E_x < 50$ MeV also gives the evidence for $Q = 0.93 \pm 0.05$, but the uncertainty of the (p, n) experiments still remains high.

The isosinglet ($T = 0$) effective *NN* interaction in the *pp* channel is assumed to have a form similar to a like-particle pairing and is characterized by the constant g'_ξ. The CQRPA equations of the FFS allow a reasonable description of nuclear spin-isospin modes for $g'_\xi = 0.2$–0.3, which is relatively far from the instability point in the *pp* channel [18].

III. RESULTS

A. β-decay half-lives

Calculations of the total β-decay half-lives have been performed for several isotopic chains with $Z \geqslant 28$. For the Ni isotopic chain, the results are displayed at Fig. 1(a) and compared with the RPA calculation based on the finite-range droplet model (FRDM) [5] and experimental data [29–32]. The FRDM+RPA calculations overestimate the experimental data and predict a strong odd-even effect in the total β-decay half-lives because of the omission of the effective *pn* interaction in the particle-particle channel. The calculation performed in the present work is in better agreement with the preliminary experimental data for Ni isotopes [29] than the one from [7]. A slight underestimate of the experimental half-lives [30–32] is observed for $A = 74$–76. It can be seen that the total half-lives in a rather long isotopic chain of $A = 71$–86 reveal a fairly regular behavior. Importantly, such a regular A dependence of the total β-decay half-lives can be described only by taking into account the forbidden decays. [When calculated in the pure GT approximation, it has a kink at $A > 79$ as shown at Fig. 1(a)]. To stress this point, we also show in Fig. 2 the isotopic dependence of the energies for the main GT and FF transitions within the Q_β window. Evidently, FF decays play a minor role for nuclei with $A \leqslant 78$ because of the low transition energies (small available phase space). In contrast, after crossing the $N = 50$ shell, the high-energy FF transitions give nonnegligible contributions to the total half-life for nuclei with $A \geqslant 79$.

The total β-decay half-lives for Cu isotopes with $A < 76$ [Fig. 3(a)] agree with the FRDM+RPA [5] calculations. For $^{76-79}$Cu, our calculation describes better the experimental data [33–39]. The forbidden decays give a dominant contribution

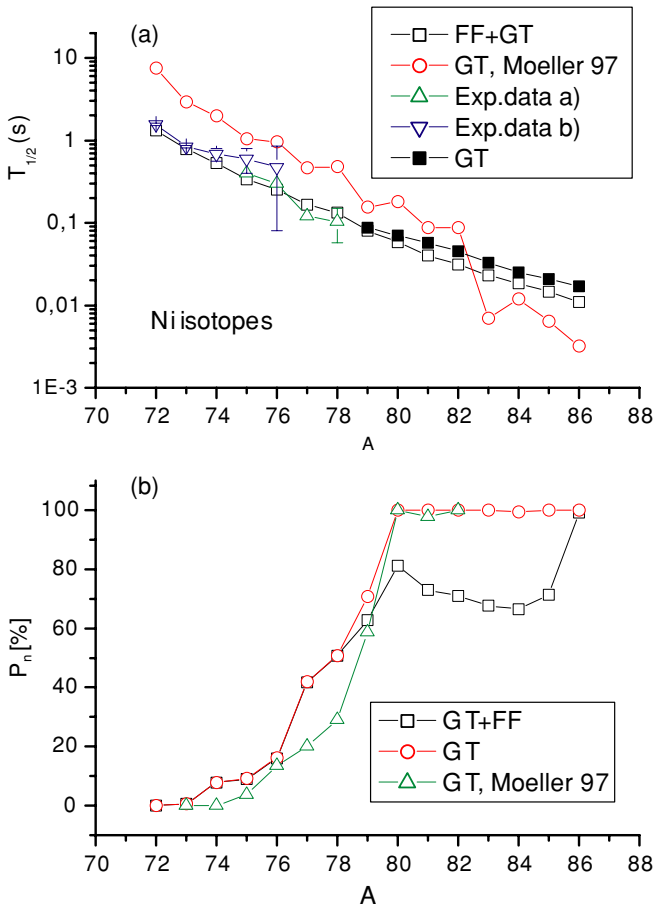

FIG. 1. (Color online) (a) Total β-decay half-lives and (b) delayed neutron emission probabilities for Ni isotopes predicted from DF3+CQRPA including the allowed (GT) plus first-forbidden (FF) transitions, and the allowed transitions, in comparison with the FRDM+RPA calculation for allowed transitions (Möller [5]) and experimental data a) [29] and b) [30–32].

to the the total half-lives for $A \geqslant 80$. For $^{76-79}$Cu for which the spherical shape is predicted, the calculation by [5] gives much shorter half-lives than the present calculation.

As for the other even-Z isotopes considered in this paper, Zn [Fig. 4(a)] and Ge [Fig. 5(a)], the calculation overestimates the experimental data available from the compilations [38,39] by about a factor of 2. Even though the deviations could be removed by using a slightly higher strength of the *pp* interaction, the *NN* interaction parameters were kept unchanged.

For the Ga isotopes with $A \leqslant 84$ [Fig. 6(a)], both our and FRDM+RPA calculations give practically a similar agreement with the experimental data [37,39]. As seen in Fig. 6(a), the FRDM+RPA calculations [5] underestimate the experimental data for $A = 84$, while our calculations overestimate them. This disagreement is related to the onset of the ground state deformation in Ga isotopes with $A \geqslant 84$. Apparently it could not be removed within the spherical approach used in our calculations.

For $^{84-86}$As [Fig. 7(a)], an underestimation of the experimental data [39] (up to a factor of 1.5) is observed. For ^{87}As, our calculation overestimates the experimental data by a factor of 2; while for $^{88-89}$As, the results are close to those estimated in [38].

B. β-delayed neutron emission

Within the allowed transitions approximation used in the global calculations [4,5], the isotopic dependence of the P_n value is rather schematic. It is mainly defined by the decay to the back spin-flip and core-polarized states often referred to as the GT pigmy resonance. Their matrix elements increase with N-Z, as well as the phase space $Q_{\beta n}$ available for the delayed neutron emission. Thus, after the GT pigmy resonance turns to be located within the $Q_{\beta n}$ window, the P_n value simply tends to the maximum. On the other hand, in the model including the different β-decay channels, an isotopic dependence of the P_n value is defined by the relative energies of the GT and FF transitions, which behave differently with increasing A. Importantly, for the neutron excess bigger than one major shell, the additional high-energy FF transitions appear.

The calculations of the β-delayed emission probabilities have been performed for several isotopic chains with $Z \geqslant 28$ [Figs. 1(b) to 6(b)]. First, let us discuss in detail the A dependence of the P_n values for Ni isotopes. It is seen in Fig. 2 that for the Ni isotopes with $A \leqslant 79$, no neutrons can be emitted following the decay to the GT pygmy resonance in the emitter nuclei. According to the present DF+CQRPA calculations, the latter is located outside the $Q_{\beta n}$ window (Fig. 2). For this reason, the increase of total delayed neutron emission probability in Ni isotopes with $A \leqslant 79$ [Fig. 1(b)] is entirely due to relatively low-energy GT and FF β decays.

Starting from $A = 79$, the GT pigmy resonance is located within the $Q_{\beta n}$ window (Fig. 2); and for a pure GT decay, the P_n values for $A \geqslant 79$ would tend to 100%. However, for the isotopes with $A \geqslant 79$ crossing the $N = 50$ shell, the relevant shell configuration space changes drastically. From Fig. 2, which also shows the energies of the different FF transitions with the total transferred momentum $J = 0$, we see that with filling of the $\nu 2d_{5/2}$ orbital in the $A \geqslant 79$ isotopes, the high-energy FF component of the β-strength function appears because of the $\nu 2d_{5/2} \rightarrow \pi 2f_{5/2}$ transition. As mentioned above, the high-energy FF transitions give a dominant contribution to the total β-decay half-lives in the Ni isotopes with $A \geqslant 79$. At the same time, their calculated energies are higher than the $Q_{\beta n}$ threshold. Hence, the high-energy part of the β-strength function does not affect the delayed neutron emission; this feature translates into a "gap"-like pattern in the $P_n(A)$ curve [Fig. 1(b)]. Notice that the $Q_{\beta n}$ value grows with A more rapidly than the GT pigmy resonance energy, and finally it becomes bigger than the FF transition energies. In such a way, for $A \geqslant 86$, the main $J = 0$ transitions are located in the $Q_{\beta n}$ window (Fig. 2), and the corresponding P_n values tend to the maximum (Fig. 4). It would be important to check our prediction for the Ni isotopic chain; though for $A \geqslant 80$ for which the difference with the GT approximation is observed, it may be difficult at the moment. The calculated P_n values for Cu isotopes are in agreement with available experimental data [36–38] [Fig. 3(b)]; the character of the isotopic dependence of the P_n values is similar to the one in Ni isotopes.

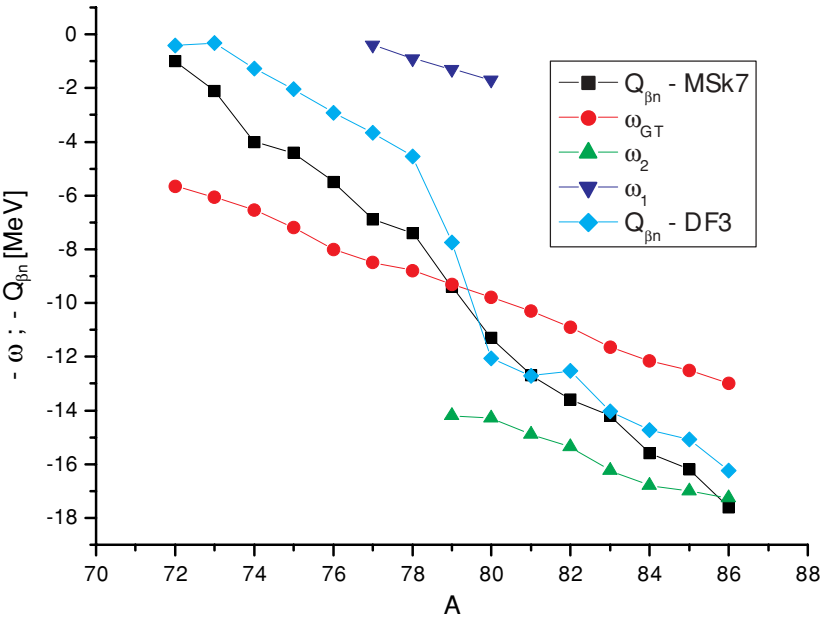

FIG. 2. (Color online) The calculated position of the $Q_{\beta n}$ window for the delayed neutron emission compared to the energies of the GT pygmy-resonance (ω_{GT}) and main $J^{\pi} = 0^{-}$ transitions ($\omega_{1,2}$) in Ni isotopes. For convenience, the transition energies and neutron emission windows are plotted with the opposite sign. A zero energy corresponds to the precursors ground states. For the lowest energy branch of the 0^{-} transitions (ω_1), only the points for $A = 77$–81 are shown.

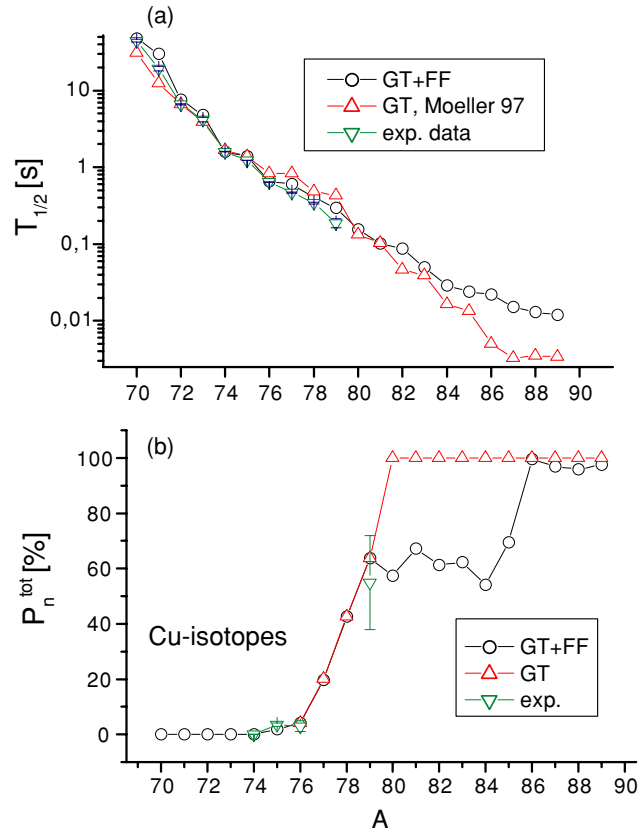

FIG. 3. (Color online) (a) Total β-decay half-lives for Cu isotopes calculated from DF3+CQRPA including the allowed and first-forbidden transitions, in comparison with the FRDM+RPA for allowed transitions [5] and experimental data [33–39]. (b) Delayed neutron emission probabilities for Cu isotopes calculated from DF3+CQRPA including the 1) allowed and first-forbidden transitions, 2) allowed transitions in comparison with the experimental data [36–39].

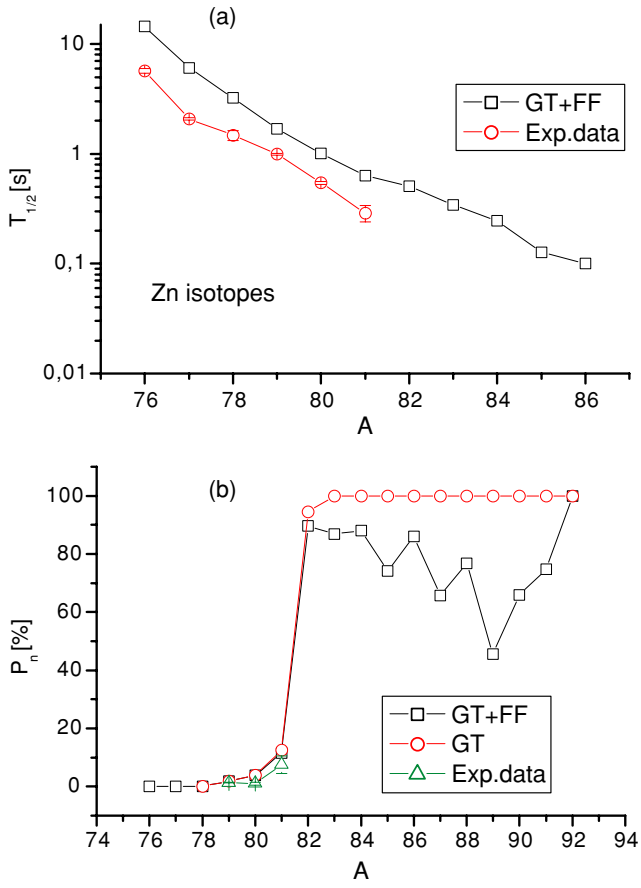

FIG. 4. (Color online) (a) Total β-decay half-lives and (b) delayed neutron emission probabilities for Zn isotopes calculated from the DF3+CQRPA including the allowed and first-forbidden transitions in comparison with the experimental data [38–39].

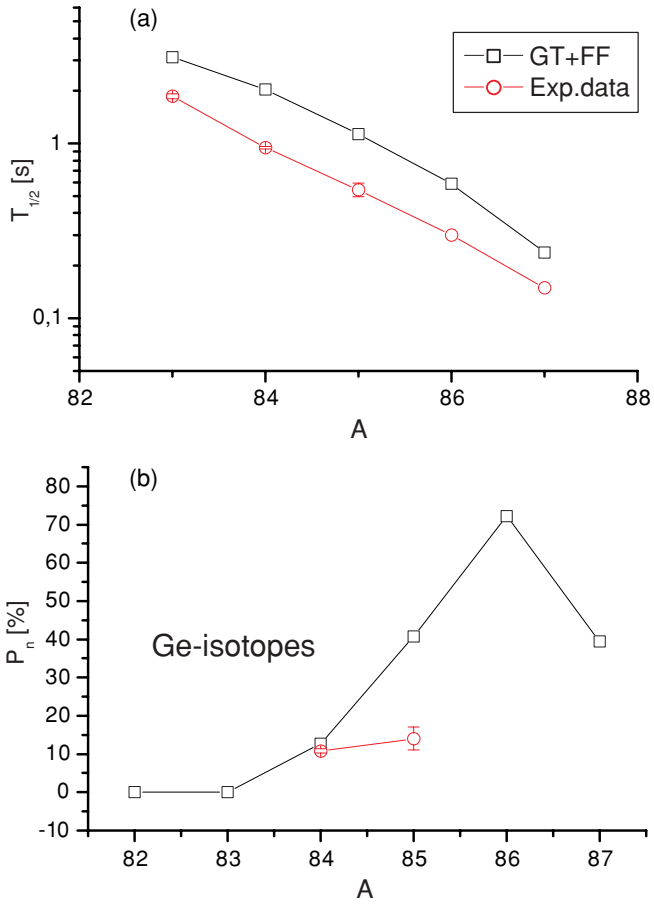

FIG. 5. (Color online) (a) Total β-decay half-lives and (b) delayed neutron emission probabilities for Ge isotopes calculated from the DF3+CQRPA including the allowed and first-forbidden transitions. The experimental data are from [39].

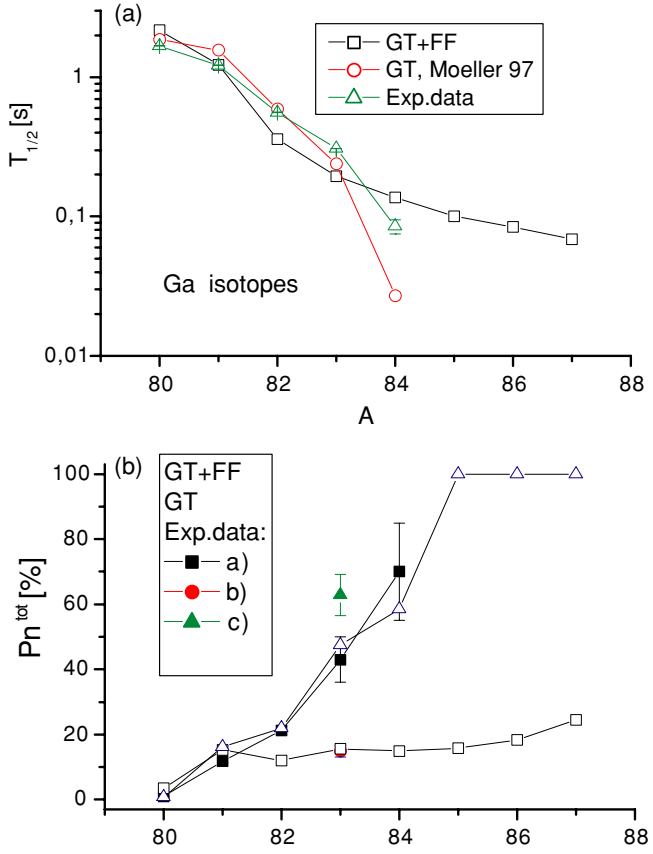

FIG. 6. (Color online) (a) Total β-decay half-lives for Ga isotopes calculated from the 1) DF3+CQRPA including the allowed and first-forbidden transitions, 2) FRDM+RPA for the allowed transitions [5] in comparison with the experimental data [39]. (b) Delayed neutron emission probabilities for Ga isotopes calculated from DF3+CQRPA: 1) including allowed and first-forbidden transitions, 2) for allowed transitions. The experimental data are taken from a) [39], b) [40], c) [41].

In the context of the possible experimental measurements, the isotopes with higher Z are of special interest. Calculations show that with filling the $2f_{7/2}$, $2p_{3/2}$ shells, the energies of the main $J = 0,1$ forbidden transitions become higher. Even though the corresponding matrix elements reduce because of the blocking of the $2f_{7/2}$, $2p_{3/2}$ levels, the overall contribution of the forbidden transitions to the total half-lives gradually increases. For even-Z isotopes of Zn and Ge, the half-lives calculated in the allowed GT approximation are on average longer by factors of 1.2–6 and 1.3–3 than the ones from the GT+FF calculations. For odd-Z Ga and As isotopes, the reduction factors are 4–8 and 4–25 respectively. Accordingly, in Zn-As isotopes [Figs. 4(b)–7(b)] the suppression of the calculated P_n values relative to the ones obtained in the GT approximation is stronger than in Ni and Cu isotopes. In Zn isotopes, an odd-even staggering of the P_n values is more prominent (it mainly reflects odd-even effects in the energies of forbidden transitions).

In Ga, Ge, and As isotopes characterized by substantial suppression of the P_n values, our calculations can be compared with existing experimental data. For $^{80-81}$Ga, the FF transitions are of minor importance, but with increasing A their contribution becomes very significant. It follows from Fig. 6(b) that in contrast with Ni and Cu isotopes, the P_n values calculated for $^{82-87}$Ga isotopes are suppressed by a factor of 4–5 compared to the ones corresponding to the GT approximation. Notice that for $^{82-84}$Ga, the evaluated P_n values [39] obtained by averaging the existing experimental data [40,41] can be described within the GT approximation alone. However, it has to be realized that the discrepancy of the experimental data is very high. Interestingly enough, in ^{83}Ga, the data from [41] agree with the GT+FF calculations. Comparison with the experimental data for Ge isotopes shows that our GT+FF calculations even overestimate the P_n value for ^{85}Ge [38,39]. For As isotopes, the calculations are in qualitative agreement with existing experimental data [39]. Assuming that the reliability of the experimental data for Ga-As isotopes has been questioned in [39], it would be of great importance to perform the new measurements for these isotopic chains.

C. Discussion

One has to mention that in the $Z = 28$ region, the delayed neutron emitter nuclei have relatively high Q_β values. For that

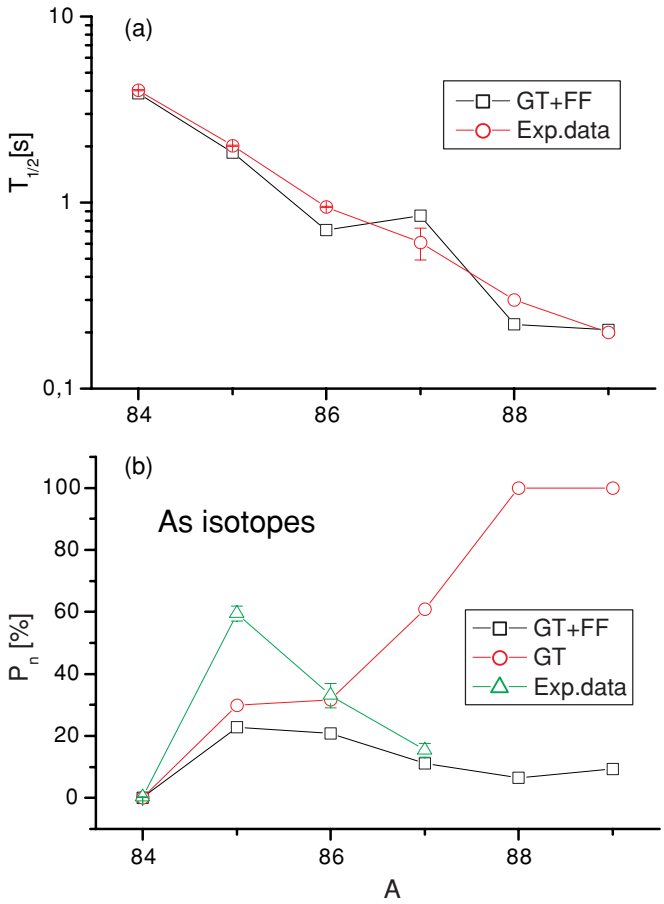

FIG. 7. (Color online) (a) Total β-decay half-lives for As isotopes calculated from the DF3+CQRPA including the allowed and first-forbidden transitions in comparison with the experimental data [39] and with estimated data for $A = 88$–89 [38]. (b) Delayed neutron emission probabilities for As isotopes calculated from (1) DF3+CQRPA including the allowed and first-forbidden transitions and (2) DF3+CQRPA including the allowed transitions. The experimental data are from [38–39].

reason, the accuracy of the calculated $T_{1/2}$ and P_n values is generally higher than for the nuclei with lower Q_β values. However, as the delayed neutron emission is typically a threshold phenomenon, it is of interest to analyze the different factors that may influence its probability. First, nuclear pairing changes the one-quasiparticle level energies and calculated B_n values. As discussed in [42], however, the only calculation was performed for ^{137}I with a very low $Q_{\beta n} = 1.6$ MeV, in which case a sensitivity to the pairing strength is extremely high. It would be important to study in detail how the predicted effect might be influenced by the different prescriptions of nuclear pairing. To roughly estimate the possible sensitivity, we varied the B_n values within ± 1 MeV. It turns out that for the nuclei with high $Q_{\beta n}$ values, the resulting impact factor is not that strong; e.g., for ^{83}Ni, the P_n value varies within the margins of 70.8% to 65.3% instead of 62.7% as shown at Fig. 1(b).

Second, the gap-like behavior of the P_n values is fairly robust against the allowed choice of the effective NN interaction parameters. (For instance, using the set of parameters corresponding to the quenching factor of $e_q = 0.8$ instead of 0.9 [7] leads to the P_n value of 71% for ^{80}Ni.)

Third, it is worth estimating the impact of the deformation and/or the specific np-nh correlations which may change the balance between the β-strengths outside and inside the $Q_{\beta n}$-window. Such an effect may be of importance if the energies of both the GT "pygmy"-resonance and FF transitions turn to lie close to the neutron emission threshold. For the nuclei of interest in $Z \approx 28$ region this is mostly not the case. In particular, for $^{80-85}$Ni for which the "gap"-effect is predicted (Fig. 2), the FF transition energy lies far from the $Q_{\beta n}$-window. Thus, an appreciable shift of the β-strength into the emission window is unlikely. Only for the nuclei near the neutron drip-line, the energies of the FF transitions are close to the $Q_{\beta - B_n}$-window but in this case the QRPA can not be applied. As for the possible impact of the deformation, the calculation [16] predicts the quasispherical shape ($\beta_2 \leqslant 0.1$) for most of the isotopes considered in the present calculations: Ni isotopes with $A = 74$–94, Cu isotopes with $A = 79$–83, Zn isotopes with $A = 86$–89, Ga isotopes with $A = 79$–83, Ge isotopes with $A = 81$–83, and As isotopes with $A = 83$–86.

Finally, as a proper account for the particle emission channels within the Hausser-Feshbach framework has not been performed, the predicted P_n values may be considered as an upper limit estimate. Moreover, for very neutron-rich nuclei the B_n values become low, as well as the density of the neutron unbound levels in the near-threshold region. In such a case, a more detailed study of the β-delayed neutron emission may be needed considering the contribution of direct neutron decay of the isobaric states.

IV. SUMMARY

The DF+CQRPA model of the delayed neutron emission is elaborated with the Gamow-Teller and first-forbidden β-decay modes taken into account. The systematic calculation of the total β-decay half-lives and delayed neutron emission probabilities has been performed for nuclei near the closed shells at $Z = 28$ and $N = 50$. Within the extended model, an agreement with the experimental data on the total half-lives is better than in our previous calculations [7]. At the same time, the available experimental data on the P_n values (see the compilations [38,39]) are described reasonably well.

For nuclei crossing the neutron shell at $N = 50$ having the neutron excess more than one major shell, a suppression is predicted of total β-delayed neutron emission probability compared to the one estimated in the GT approximation. A threshold character of the delayed neutron emission makes it sensitive to the high-energy forbidden β-decay transitions which are found to give a significant contribution to the total half-lives. Going beyond the allowed transitions approximation reduces the total delayed neutron emission probability, as the calculated energies of the main FF transitions in $Z \approx 28$, $N > 50$ nuclei are systematically higher than the $Q_{\beta n}$ values.

A typical signature of the high-energy first-forbidden decays are the gap-like patterns in the A dependence of the total delayed neutron emission probability, like the ones seen for Ni and Cu nuclei above the $N = 50$ shell. However, in these

isotopes, the scale of predicted reduction of the P_n values is at the edge of the experimental precision currently achievable with isotope-separated beams. A stronger suppression of the P_n values predicted for Zn-As isotopic chains provides a certain challenge, as these isotopes are more accessible for experimental measurements in the short term at the ALTO (IPN, Orsay) and ISOLDE (CERN) facilities [43]. Similar reduction and staggering of the P_n values exist in nuclei above the $Z = 50$, $N = 82$ shells. In this region, the effect is even stronger, as the blocking of the $\pi 1g_{9/2}$ orbital suppresses the competing high-energy GT transitions [12] (detailed calculations for the nuclei near the neutron closed shells at $N = 82$ and 126 can be found in our recent paper [44]).

Note added in proof: Very recently the final experimental half-lives have been published for $^{75-78}$Ni isotopes by P. T. Hosmer *et al*. [45]. These experimental data and the corresponding results of our GT+FF calculation are as follows [see also Fig. 1(a)]: 344^{+20}_{-24} ms and 340 ms for ^{75}Ni; 238^{+15}_{-18} ms and 255 ms ^{76}Ni; 128^{+27}_{-33} ms and 166 ms ^{77}Ni; 110^{+100}_{-60} ms and 133 ms ^{78}Ni.

ACKNOWLEDGMENTS

The author thanks the OSTC, Belgium, for support within the PAI Program IAP P5/07 "Exotic Nuclei for Nuclear Physics and Astrophysics." Numerous discussions with M. Arnould, S. Goriely, J. M. Pearson, P. Van Duppen, M. Huyse, D. Pauwels, N. Severijns, and J.-Ch. Thomas are gratefully acknowledged.

[1] V. I. Mishin *et al*., Nucl. Instrum. Methods Phys. Res. B **73**, 550 (1993); P. Van Duppen, *ibid*. B **73**, 66 (1997); K.-L. Kratz, in *ENAM 98*, edited by B. M. Sherill *et al*., AIP Conf. Proc. No. **455** (AIP, Woodbury, NY, 1998), p. 827.
[2] H. V. Klapdor and C. O. Wene, J. Phys. G **6**, 1061 (1980).
[3] J. Blomquist, M. Kerek, and B. Fogelberg, Z. Phys. A **314**, 199 (1983).
[4] M. Hirsh, A. Staudt, and H. V. Klapdor-Kleingrothaus, At. Data Nucl. Data Tables **51**, 243 (1992).
[5] P. Möller, J. R. Nix, and K.-L. Kratz, At. Data Nucl. Data Tables **66**, 131 (1997).
[6] H. Homma *et al*., Phys. Rev. C **54**, 2972 (1996).
[7] I. N. Borzov, Phys. Rev. C **67**, 025802 (2003).
[8] H. DeWitte *et al*., Phys. Rev. C **69**, 044305 (2004).
[9] A. Pappas and T. Sverdrup, Nucl. Phys. **A188**, 48 (1972).
[10] L. N. Zyryanova, *Unique Beta Transitions*, Russ. original (Acad. Science USSR, Moscow-Leningrad, 1960); *Once Forbidden Beta Transitions*, transl. (Pergamon, New York, 1963).
[11] N. B. Gove and M. J. Martin, At. Data Nucl. Data Tables **10**, 206 (1971).
[12] I. N. Borzov *et al*., Z. Phys. A **355**, 117 (1996).
[13] S. A. Fayans *et al*., Nucl. Phys. **A676**, 49 (2000).
[14] A. B. Migdal, *Theory of Finite Fermi Systems and Atomic Nuclei Properties*, Russ. original, 2nd ed. (Nauka, Moscow, 1983).
[15] K. A. Mezilev *et al*., Phys. Scripta **T56**, 272 (1975).
[16] S. Goriely, F. Tondeur, and J. M. Pearson, At. Data Nucl. Data Tables **77**, 311 (2000).
[17] A. Bulgac, Phys. Rev. C **65**, 051305(R) (2002).
[18] I. N. Borzov and E. L. Trykov, Izv. Acad. Nauk. SSSR, Ser. Fiz. **53**, 2178 (1989).
[19] I. N. Borzov, S. A. Fayans, and E. L. Trykov, Nucl. Phys. **584**, 335 (1995).
[20] I. N. Borzov, E. L. Trykov, and S. A. Fayans, Sov. J. Nucl. Phys. **52**, 627 (1990).
[21] A. P. Platonov and E. E. Saperstein, Nucl. Phys. **A486**, 63 (1988).
[22] G. F. Bertsch, P. F. Bortignon, and R. Broglia, Rev. Mod. Phys. **55**, 287 (1983).
[23] A. Bohr and B. Mottelson, *Nuclear Structure* (Addison-Wesley, New York, 1969), Vol. I.
[24] N. I. Pyatov and S. A. Fayans, Part. Nucl. **14**, 401 (1983).
[25] K. Kubodera, J. Delorme, and M. Rho, Phys. Rev. Lett. B **40**, 755 (1978).
[26] R. U. Khafizov and S. V. Tolokonnikov, Phys. Lett. **B153**, 353 (1985); **B162**, 21 (1985).
[27] I. N. Borzov, E. E. Saperstein, S. V. Tolokonnikov, and S. A. Fayans, Part. Nucl. **12**, 848 (1981).
[28] T. Wakasa *et al*., Phys. Rev. C **55**, 2909 (1999).
[29] H. Schatz *et al*., reported in the talk of H. Schatz at ENAM 04, (2004), www.phy.ornl.gov/enam04.
[30] S. Franchoo *et al*., Phys. Rev. Lett. **81**, 3100 (1998).
[31] P. L. Reeder *et al*., Phys. Rev. C **31**, 1032 (1985).
[32] F. Ameil *et al*., Eur. Phys. J. **A1**, 275 (1998).
[33] L. Weissman *et al*., Phys. Rev. C **65**, 024315 (2002).
[34] J. I. Priscandaro *et al*., Phys. Rev. C **60**, 54307 (1999).
[35] E. Runte *et al*., Nucl. Phys. **A399**, 399 (1983).
[36] K.-L. Kratz *et al*., Z. Phys. A **340**, 419 (1991).
[37] P. L. Reeder *et al*., Research Rept. PNL-SA-14026, 1986 (unpublished).
[38] G. Audi, O. Bersillon, J. Blachot, and A. H. Wapstra, Nucl. Phys. **A729**, 3 (2003).
[39] G. Rudstam, K. Aleklett, and L. Sihver, At. Data Nucl. Data Tables **53**, 1 (1993).
[40] E. Lund *et al*., Z. Phys. A **294**, 233 (1980).
[41] P. L. Reeder *et al*., Proceedings Am. Soc. Nucl. Chem. Meeting, Chicago, 1985, p. 171.
[42] D. S. Delion, D. Santos, and P. Schuk, Phys. Lett. **B398**, 1 (1997).
[43] S. Franchoo (private communication); U. Köster (private communication).
[44] I. N. Borzov, Nucl. Phys. A (to be published).
[45] P. T. Hosmer *et al*., Phys. Rev. Lett. **94**, 112501 (2005).